

HSTrack: Bootstrap End-to-End Multi-Camera 3D Multi-object Tracking with Hybrid Supervision

Shubo Lin^{1, 2}, Yutong Kou², Bing Li^{1, 2}, Weiming Hu^{1, 2, 3}, Jin Gao^{1, 2, *}

¹State Key Laboratory of Multimodal Artificial Intelligence Systems (MAIS), CASIA

²School of Artificial Intelligence, University of Chinese Academy of Sciences

³School of Information Science and Technology, ShanghaiTech University

{linshubo2023, kouyutong2021}@ia.ac.cn, {bli,wmhu,jin.gao}@nlpr.ia.ac.cn

Abstract

In camera-based 3D multi-object tracking (MOT), the prevailing methods follow the *tracking-by-query-propagation* paradigm, which employs track queries to manage the lifecycle of identity-consistent tracklets while object queries handle the detection of new-born tracklets. However, this intertwined paradigm leads the inter-temporal tracking task and the single-frame detection task utilize the same model parameters, complicating training optimization. Drawing inspiration from studies on the roles of attention components in transformer-based decoders, we identify that the dispersing effect of self-attention necessitates object queries to match with new-born tracklets. This matching strategy diverges from the detection pre-training phase, where object queries align with all ground-truth targets, resulting in insufficient supervision signals. To address these issues, we present HSTrack, a novel plug-and-play method designed to co-facilitate multi-task learning for detection and tracking. HSTrack constructs a parallel weight-share decoder devoid of self-attention layers, circumventing competition between different types of queries. Considering the characteristics of cross-attention layer and distinct query types, our parallel decoder adopt one-to-one and one-to-many label assignment strategies for track queries and object queries, respectively. Leveraging the shared architecture, HSTrack further improve trackers for spatio-temporal modeling and quality candidates generation. Extensive experiments demonstrate that HSTrack consistently delivers improvements when integrated with various query-based 3D MOT trackers. For example, HSTrack improves the state-of-the-art PF-Track method by +2.3% AMOTA and +1.7% mAP on the nuScenes dataset.

Introduction

The perception system is an indispensable component in autonomous driving. Within the system, consistent and accurate 3D multi-object tracking (MOT) provides reliable observations for prediction and planning. Camera-based algorithms have raised significant attention due to their cost-effectiveness (Hu et al. 2023a; Scheidegger et al. 2018). Since *identity-aware* tracking is largely reliant on *identity-agnostic* detection, this has prompted many works (Zhang et al. 2022a; Pang et al. 2023; Li et al. 2023c; Ding et al. 2024) to focus on the design of paradigms that extend from

*Corresponding author.

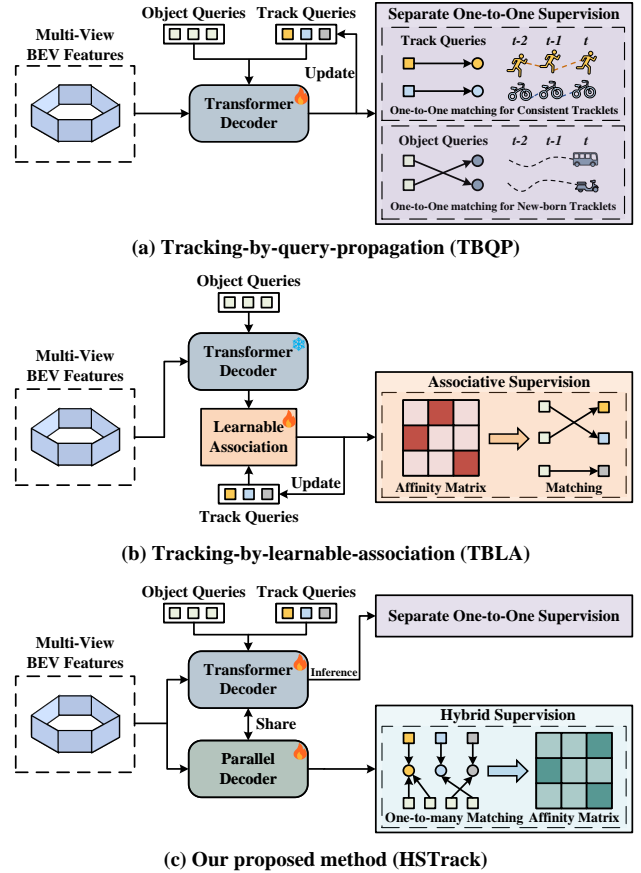


Figure 1: Paradigm-level comparison. Our proposed method (Fig. 1c) effectively transforms the decoupled associative learning of the *tracking-by-learnable-association* paradigm (Fig. 1b) into enhanced auxiliary supervision, thus moderating the representation conflicts in single query of the *tracking-by-query-propagation* paradigm (Fig. 1a).

detection to tracking. In multi-view 3D object detection, research is primarily bifurcated into dense Bird’s-Eye View (BEV)-based (Huang et al. 2022; Li et al. 2023a, 2022) and sparse query-based algorithms (Wang et al. 2021; Liu et al. 2022, 2023; Wang et al. 2023). Inspired by the advances in

Transformers for object detection, sparse query-based detectors (Wang et al. 2021; Liu et al. 2022, 2023; Wang et al. 2023) employ object queries to interact with multi-view image features and encode each object independently. These object-centric detectors have been naturally extended to identity-aware multi-object tracking algorithms.

One paradigm for this extension allows track queries to alternately propagate and update, tracking targets with the same identity cross frames, while the object query detect new-born targets, referred to as *tracking-by-query-propagation* (TBQP, Fig. 1a) (Wang et al. 2021; Pang et al. 2023; Ding et al. 2024). Both queries are separately matched with distinct tracklets based on one-to-one label assignment. However, this combined design complicates the training process. On one hand, tracking models are typically initialized with pre-trained weights of detection. In the pre-training stage for single-frame detection, object queries are matched with all ground-truth targets, which inherently enables the object queries to consistently detect targets that persist. The propensity of object queries to match new-born objects not only reduces the supervision signals but also tends to confuse the model. On the other hand, a single query embedding perform both intra-temporal detection and inter-temporal association, which is difficult to optimize since both tasks share the same network parameters.

Another paradigm for the extension of query-based MOT decouples detection and tracking, known as *tracking-by-learnable-association* (TBLA) (Li et al. 2023c; Ding et al. 2023). As illustrated in Fig. 1b, TBLA freezes the parameters of detector, allowing a differentiable learnable module to associate both queries and utilizing the matched object query to update track query. However, TBLA not only restricts the learning of object feature in detector but also limits the spatio-temporal modeling in tracker.

This paper, from the perspective of optimizing training efficiency, aims to reconsider the relationship between detection and tracking in the *tracking-by-query-propagation* paradigm at a granular level. Drawing inspiration from works (Hu et al. 2023b; Jia et al. 2023), we conduct a detailed analysis of the components in the transformer-based decoder: the standard decoder layers include self-attention, cross-attention, and FFNs. The role of cross-attention is to dynamically aggregate multi-view image features, resulting in duplicate candidates for object queries and allowing track queries to model temporal context for iterative updates. The aggregation also closes the feature distance among queries around a single target. The role of self-attention is to de-duplicate candidates from both object queries and track queries, dispersing queries far away from each other.

Based on the analysis, we argue that the dispersing effect of self-attention, forcibly isolating object queries from track queries, is sub-optimal. This not only causes the supervision of object queries to be inconsistent between detection pre-training and tracking fine-tuning, but also hinders the effective association between track queries and object queries. To address these issues, we present HSTrack, a novel plug-and-play method for end-to-end multi-camera 3D MOT framework that constructs a parallel weight-share decoder with hybrid supervisions for distinct queries, as il-

lustrated in Fig. 1c. The parallel decoder removes all self-attention layers from the standard decoder. During tracking fine-tuning, both types of queries are collaboratively fed into the two decoders. The standard decoder still uses separate one-to-one supervision for both queries, while the parallel decoder uses one-to-one supervision for track queries and one-to-many supervision for object queries. This decoupled assignment in the parallel decoder ensures that track queries maintain identity-aware characteristics in spatio-temporal modeling, while object queries obtain more and better candidates representations. Subsequently, query association is employed between object queries and track queries to construct the affinity matrix. We treat pairs of queries matched to the same ground-truth targets as positive samples and others as negative samples, constructing bidirectional associative supervision. In this way, the auxiliary associative supervision enables the two types of queries to learn from each other and gain more useful information, thus harmonizing both detection and tracking.

We conduct extensive experiments with multiple *tracking-by-query-propagation* paradigm methods to validate the effectiveness of HSTrack. Experimental results show that HSTrack significantly enhances the performance of both detection and tracking for end-to-end multi-view 3D MOT trackers. Specifically, HSTrack achieves +2.3% improvement in AMOTA and +1.7% improvement in mAP combined with the state-of-the-art PF-Track method on the nuScenes dataset.

Related Work

Tracking by association

Tracking-by-association paradigm decouples detection and tracking, regarding tracking as a post-processing step following object detection. The conventional workflow (Weng et al. 2020a; Pang, Li, and Wang 2022; Zhang et al. 2022b; Wojke, Bewley, and Paulus 2017) first detects objects in each frame with accurate detector. Subsequently, the detected objects are associated with existing trajectories. by handcraft features such as appearance similarity (Hu et al. 2023a; Wojke, Bewley, and Paulus 2017), geometric distance (Yin, Zhou, and Krähenbühl 2021; Bai et al. 2022; Zhou, Wang, and Krähenbühl 2019), and IoU (Weng et al. 2020a; Pang, Li, and Wang 2022). To achieve one-to-one associations between detected objects and existing trajectories, Hungarian (Kuhn 2010) or greedy matching are often applied. Tracking-by-association paradigm achieves further advancements when combined with query-based detectors. Specifically, learning modules such as GNN (Weng et al. 2020c; Weng, Yuan, and Kitani 2021), LSTM (Hu et al. 2023a; Marinello, Proesmans, and Gool 2022), and Transformers (Zeng et al. 2021) are employed to merge multi-faceted information. However, detection and tracking are complementary yet non-independent tasks. This partitioned paradigm design does not effectively optimize both tasks simultaneously.

Tracking by query propagation

Another methods that extend query-based detectors for tracking treat MOT as a multi-frame set prediction problem (Zeng et al. 2022; Sun et al. 2020). *Tracking-by-query-propagation* jointly performs detection and tracking auto-regression by using object-centric latent encodings from the previous frame as priors (track queries) for the next frame. MUTR3D (Zhang et al. 2022a) extends MOTR-style trackers to multi-view 3D MOT based on the DETR3D detector, compensating for object position in consecutive frames by integrating both object and ego motion linear adjustments using velocity predictions and reference points of each object. STAR-Track (Doll et al. 2024) introduces a Latent Motion Model (LMM) to account for changes in query appearance features across frames. PF-Track (Pang et al. 2023) consolidates detection, tracking, and prediction by constructing memory bank to optimize queries and bounding boxes and predict trajectory motion for long-term tracking. ADA-Track (Ding et al. 2024) incorporates a query-to-query cross-correlation module, which integrates clues that match the appearance and geometric features of the track queries into the dynamic attention map to refine object queries. Our work is orthogonal to these end-to-end methods and can be seamlessly integrated into the training of *tracking-by-query-propagation* paradigm without introducing extra modules.

Hybrid supervision

Hybrid supervision is common in techniques such as deep supervision (Lee et al. 2015) and multi-task learning (Zhang et al. 2014; Dai, He, and Sun 2016). In object detection, early CNN-based detectors (Ren et al. 2017; Jiang et al. 2018; Redmon and Farhadi 2018) employed dense predictions across multiple resolution levels and incorporated hybrid supervision. With the advent of DETR (Carion et al. 2020; Zhu et al. 2021), many studies have developed hybrid supervision methods aiming to improve the training efficiency of DETR-style detectors through techniques like denoising (Li et al. 2024), grouped queries (Chen et al. 2023), and parallel decoders (Hu et al. 2023b). In multi-view 3D tracking algorithms, the absence of depth information (Li et al. 2023b) prevents accurate projection of each pixel in 3D space, limiting the model’s representational capacity under sparsely activated one-to-one supervision. Although tracking and detection are interdependent, they possess distinct characteristics. Hence, we regard end-to-end tracking as a multi-task optimization problem, further breaking down sub-problems by constructing the parallel decoder.

Methodology

The framework of HSTrack is conceptually simple: In the inference stage, HSTrack follows the *tracking-by-query-propagation* paradigm. In the training stage, HSTrack employs a parallel encoder that omits all self-attention layers, while sharing the remaining decoder parameters. The track queries and object queries produced by the parallel encoder are supervised using one-to-one and one-to-many label assignment strategies, respectively. Finally, query association is utilized to construct the affinity matrix for the two types

of queries, with identity-guided supervision. The architecture of HSTrack is illustrated in Fig. 2. In this section, we delve into the workflow and provide a detailed exposition.

Preliminaries

The initial *tracking-by-query-propagation* paradigm model consists of a backbone (e.g., ResNet (He et al. 2016), VoVNet (Lee et al. 2019)), a transformer-based decoder, and predictors for object class and boxes. Given N images $\mathbf{I}_t = \{\mathbf{I}_t^i \in \mathbb{R}^{3 \times H_c \times W_c}, i = 1, 2, \dots, N\}$ captured by surrounding cameras at timestamp t , the goal of 3D MOT is to generate detection boxes of the instances in the perceptual scene with consistent IDs. First, images are processed through the backbone to extract multi-view image features. Subsequently, either 3D-to-2D projection sampling (Wang et al. 2021) or 2D-to-3D positional embedding (Liu et al. 2022; Wang et al. 2023) is employed to generate the final encoder output, denoted as φ .

$$\mathbf{F}_t^{2d} = \text{Backbone}(\mathbf{I}_t), \mathbf{F}_t^{3d} = \varphi(\mathbf{F}_t^{2d}, \mathbf{Pos}) \quad (1)$$

where \mathbf{F}_t^{2d} and \mathbf{F}_t^{3d} are 2D multi-view features and 3D position-aware features, respectively. \mathbf{Pos} represents predefined BEV space positional information. The key point in realizing end-to-end tracking is to allow the prior latent encoding from previous frame, track queries \mathbf{Q}_{t-1}^T , to be updated iteratively by the decoder interacting with the current frame image features. To detect new-born targets, object queries \mathbf{Q}^O with fixed number of \mathbf{N}_O are merged together and fed into the decoder:

$$\mathbf{Q}_t^T, \mathbf{Q}_t^O = \text{Decoder}(\mathbf{F}_t^{3d}, \text{concat}(\mathbf{Q}_{t-1}^T, \mathbf{Q}^O)) \quad (2)$$

Each query $q \in \{\mathbf{Q}^T, \mathbf{Q}^O\}$ includes an embedding vector e_i , assigned with a unique 3D reference c , i.e., $q = \{e, c\}$. In the center-point anchor-free predictors, the reference points of queries are actively involved in the parsing of the bounding box:

$$\mathbf{B}_t = \text{box}_{1 \rightarrow 1}(e_t, c_t), \mathbf{P}_t = \text{cls}_{1 \rightarrow 1}(e_t) \quad (3)$$

where $\mathbf{B}_t = \{b : [\tilde{c}, s, \theta, v] \in \mathbb{R}^9\}$ is the set of prediction 3D boxes and $\mathbf{P}_t = \{p \in \mathbb{R}^{\mathbf{N}_c}\}$ is the set of classification scores for all categories (\mathbf{N}_c). Each box (b) consists of 3D center point ($\tilde{c} \in \mathbb{R}^3$), 3D box size ($s \in \mathbb{R}^3$), yaw angle ($\theta \in \mathbb{R}^1$), and BEV velocity ($v \in \mathbb{R}^2$). For brevity, we use subscript $1 \rightarrow 1$ and $1 \rightarrow m$ to denote the one-to-one and one-to-many label assignment strategies.

Finally, the estimation of the reference points for both queries is refined to obtain a more accurate spatial positional prior in the next frame. Specifically, the BEV velocity v_t^i , and the 3D center point \tilde{c}_t^i , of the i_{th} instance are extracted from box. Based on the constant velocity motion assumption, we predict the 3D center point of the instance for frame $t + 1$ in BEV space: $\tilde{c}_t^i = \tilde{c}_t^i + v_t^i \Delta t$, where Δt represents the time interval between successive frames. The predicted 3D center point is then transformed to the new vehicle coordinate system through ego-motion compensation.

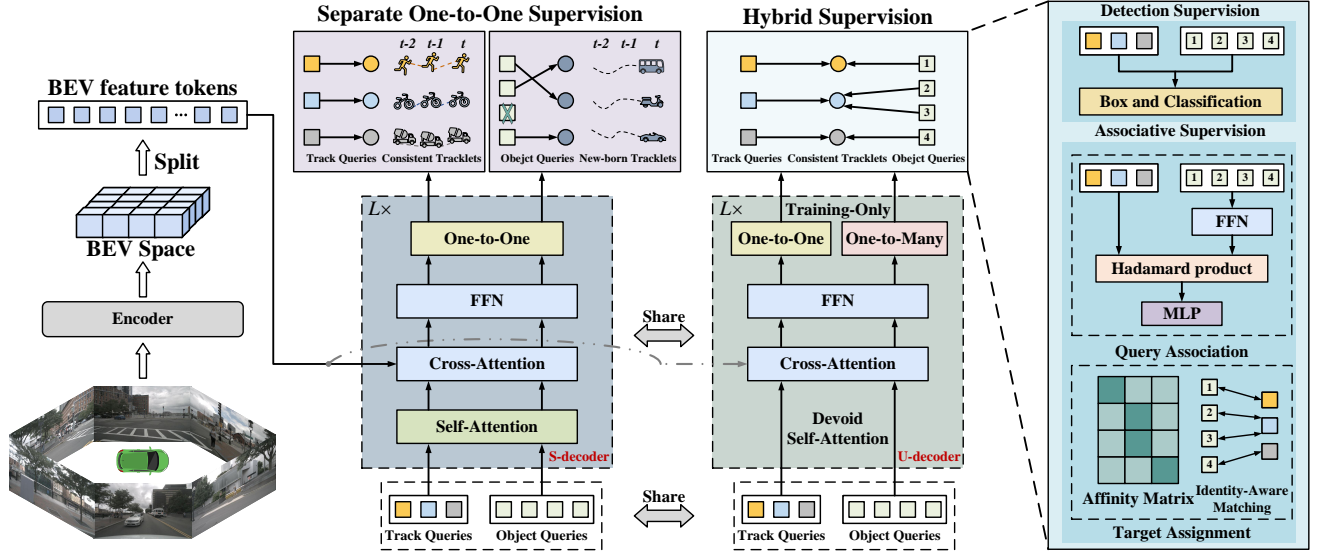


Figure 2: Overview of HSTrack. HSTrack follows the encoder-decoder architecture, with two weight-share parallel decoders: a S-decoder (standard decoder) and an U-decoder (devoid of self-attention layers). Both transformer-based decoders take BEV feature tokens, decoupled object queries and track queries as input. In the S-decoder, we adopt a one-to-one label assignment strategy, where object queries and track queries are matched to new-born tracklets and consistent tracklets, respectively. In the U-decoder, we match object queries with consistent tracklets for one-to-many matching, while the assignment of track queries remains unchanged. Then query association is applied to construct the affinity matrix between object queries and track queries. Through the identity-guided matching of these two query types, associative supervision is conducted to collectively enhance the learning of representations for both detection and tracking.

Hybrid Supervisions

HSTrack follows the workflow of the *tracking-by-query-propagation* paradigm by constructing a parallel decoder branch which removes all self-attention layers in the training stage. To further strengthen the cross-temporal modeling capability of track queries and improve the representation quality of object query candidates, we implement one-to-one and one-to-many label matching for track queries and object queries, respectively. Tracking and object queries assigned to the same label form an associative supervision, enabling the models to mutually benefit during multi-task optimization.

Parallel Decoders

We design two parallel decoders: a standard decoder (S-decoder) and a decoder without self-attention layers (U-decoder). A block in the standard decoder consists of a self-attention layer, a cross-attention layer and a feed-forward network (FFN). The embeddings of both object and track queries are concatenated and fed into the two decoders, denoted as e_s^l and e_c^l . The superscript $l = \{0, 1, \dots, 5\}$ indicates the index of the decoder block and we omit the notation of the frame index t for simplicity. The initial inputs to both decoders are identical, i.e., $e_s^0 = e_c^0$. In the l_{th} block of the S-decoder, the state information of both queries is first updated through the self-attention layer bidirectionally:

$$\hat{e}_s^l = e_s^l + \text{SA}(Q = K = V = e_s^l) \quad (4)$$

where $\text{SA}(\cdot)$ indicates the self-attention layer. Next, the two types of queries are interplayed with multiview image

features, where object queries generate potential candidates through the positional priors, and track queries locate successive targets using discriminative representation prior:

$$e_s^{l+1} = \text{FFN}(\hat{e}_s^l + \text{CA}(Q = \hat{e}_s^l, K = V = \mathbf{F}^{3d})) \quad (5)$$

where $\text{CA}(\cdot)$ indicates the cross-attention layer. The U-decoder retains the cross-attention layers and FFNs, sharing parameters with the S-decoder. In this setup, the cross-attention layers take image features as the sole source set (key and value), dynamically aggregating and updating both queries in the stacked decoder blocks:

$$e_u^{l+1} = \text{FFN}(e_u^l + \text{CA}(Q = e_u^l, K = V = \mathbf{F}^{3d})) \quad (6)$$

Lacking the mutual interaction of self-attention layers, it is challenging for U-decoder to remove duplicate candidates with similar distances in the high-dimensional embedding space. Thus, we design distinct label assignment strategies tailored to the characteristics of the two parallel decoders and the specific requirements of their respective tasks.

Target assignment

In the S-decoder, we follow the bipartite label matching strategy of the *tracking-by-query-propagation* paradigm: track queries are matched with ground-truth targets that have consistent identities, $\bar{\mathbf{Y}}_{t,c} = \{y_{t,c}^i : [\bar{b}_t^i, \bar{p}_t^i, id_t^i], id_t^i = id_{t-1}^i\}$, while object queries are matched with the remaining new-born ground-truth targets, $\bar{\mathbf{Y}}_{t,n} = \{\bar{y}_{t,n}^i :$

$[\bar{b}_t^i, \bar{p}_t^i, id_t^i], id_{t-1} \in \emptyset\}$, utilizing the Hungarian algorithm. Each query corresponds to a ground-truth target and vice versa. The track queries corresponding to disappearing targets are not assigned labels.

In the U-decoder, we maintain the identity-guided principle for track queries, but perform one-to-many greedy matching for object queries with consistent ground-truth targets $\bar{Y}_{t,cs}$, i.e., one ground-truth target corresponds to multiple object queries. The two types of queries are fed into the shared predictor and supervised in a hybrid manner according to the assigned labels:

$$\mathbf{B}_u^O = \text{box}_{1 \rightarrow m}(e_u^O, c_u^O), \mathbf{P}_c^O = \text{cls}_{1 \rightarrow m}(e_u^O) \quad (7)$$

$$\mathbf{B}_u^T = \text{box}_{1 \rightarrow 1}(e_u^T, c_u^T), \mathbf{P}_u^O = \text{cls}_{1 \rightarrow 1}(e_u^T) \quad (8)$$

Specifically, one-to-many matching is based on the matching cost between U-decoder’s prediction $\mathbf{B}_u, \mathbf{S}_u$ and the consistent ground-truth \bar{Y}_c . For the i_{th} ground-truth target and the j_{th} prediction, the matching cost $\mathbf{MC}_{i,j}$ is calculated as follows:

$$\mathbf{MC}_{i,j} = \text{FocalLoss}(\bar{p}_{cs}^i, p^j) + \text{L1}(\bar{b}_{cs}^i, b_u^j) \quad (9)$$

After obtaining the query-to-ground-truth cost pairs, we filter out unreliable matching pairs whose cost exceeds the threshold τ . Then, for each ground-truth target, we select the bottom k queries to assign the same label. In order to obtain more positive sample pairs in subsequent associative supervision, we do not match object queries with all ground-truth targets. In subsequent section, we explore the impact of different label assignment strategy variants in detail.

Query association

In the U-decoder, one-to-many label assignment strategy allows partial object queries and track queries match to the same ground-truth target. To further obtain discriminative latent encoding, we supervise the association of both types of queries assigned to the same target by constructing the affinity matrix. Specifically, we feed the object query embeddings e_u^O into a FFN to generate distinct appearance features $\tilde{e}_u^O \in \mathbb{R}^{N \times C}$, aligned with the cross-frame track query embeddings $e_u^T \in \mathbb{R}^{M \times C}$, where C denotes the embedding channels. We calculate query-to-query features $\mathbf{F}_u \in \mathbb{R}^{N \times M \times C}$ between \tilde{e}_u^O and e_u^T using Hadamard product. Finally, we utilize a multi-layer perception (MLP) to predict the affinity matrix $\tilde{\mathbf{F}}_u \in \mathbb{R}^{N \times M}$, following by a softmax function. The entire association process is formulated as follows:

$$\tilde{\mathbf{F}}_u = \text{softmax}(\text{MLP}(\text{FFN}(e_u^T) \odot e_u^O)) \quad (10)$$

Our associative supervision does not rely on motion or geometric cues. Instead, it aims to enable the learning of enriched representations from both types of queries in a bidirectional manner. At the first frame there are no track queries yet, so we skip the parallel decoder for $t = 1$.

Loss function

Following (Wang et al. 2021; Liu et al. 2022), we use Focal Loss (Lin et al. 2020) for classification score and ℓ_1 -loss for box regression. For track queries, one-to-one supervision with consistent ground-truth targets is implemented in both parallel decoders. Object queries still implement one-to-one supervision with new-born ground-truth targets in the S-decoder, but use one-to-many supervision with consistent ground-truth targets based on matching cost in the U-decoder. For the intermediate layer outputs of the two parallel decoders, we also construct auxiliary loss for all mentioned items. Regarding the associative supervision of the affinity matrix in Equation (10), we establish the optimization target \bar{Y}_{asso} based on the identity correspondence of the two queries. We formulate the cross-entropy loss for the affinity matrix to correctly categorize each object query into track queries with the same identity, i.e. $L_{asso} = CE(\bar{Y}_{asso}, \tilde{\mathbf{F}}_u)$. Training optimization is performed on a continuous sequence clip with K frames, where the loss for object queries is computed from the first frame, while the loss for track queries and the association are computed from the second frame onward. The loss for the entire sequence can be formulated as follows:

$$\mathcal{L}_T = \mathcal{L}_{1 \rightarrow 1}(\bar{p}_c, \bar{b}_c, p_s^T, b_s^T) + \mathcal{L}_{1 \rightarrow 1}(\bar{p}_c, \bar{b}_c, p_u^T, b_u^T) \quad (11)$$

$$\mathcal{L}_D = \mathcal{L}_{1 \rightarrow 1}(\bar{p}_n, \bar{b}_n, p_s^O, b_s^O) + \mathcal{L}_{1 \rightarrow m}(\bar{p}_c, \bar{b}_c, p_u^O, b_u^O) \quad (12)$$

$$\mathcal{L} = \sum_{t=1}^K \lambda_{Det} \mathcal{L}_D^t + \sum_{t=2}^K (\lambda_{Track} \mathcal{L}_T^t + \lambda_{asso} \mathcal{L}_{asso}^t) \quad (13)$$

where λ_{Det} , λ_{Track} , and λ_{asso} represent the loss coefficients for detection, tracking, and association, respectively, all of which are set to 1.0 by default.

Experiments

Experimental Setup

Dataset

We evaluate our approach on the nuScenes dataset (Caesar et al. 2020), a large-scale benchmark for autonomous driving, which contains 700, 150, and 150 scenes for training, validation, and testing, respectively. Each scene spans roughly 20 seconds with multi-modal synchronized data captured from LiDAR, RADAR and six cameras providing a 360° field of view. In this paper, we use camera sensors only. The dataset is annotated with key-frames at a frequency of 2Hz and covers 10 types of common objects on the road. For the tracking task, nuScenes selects a subset of 7 movable categories, excluding static objects such as traffic cones.

Metrics

Consistent with official evaluation metrics for multi-object tracking tasks on nuScenes, we primarily report AMOTA (average multi-object tracking accuracy) and AMOTP (average multi-object tracking precision) (Weng

Method	Detector	Tracking						Detection		
		AMOTA \uparrow	AMOTP \downarrow	Recall \uparrow	MOTA \uparrow	IDS \downarrow	FP \downarrow	FN \downarrow	NDS \uparrow	mAP \uparrow
MUTR3D (Ding et al. 2024)	DETR3D	32.1%	1.448	45.2%	28.3%	474	15269	43828	-	-
HSTrack(ours)	DETR3D	34.0%	1.441	45.4%	30.4%	578	14382	42813	-	-
PF-Track-S (Pang et al. 2023)	PETR	40.8%	1.343	50.7%	37.6%	166	15288	40398	47.7%	37.8%
HSTrack (ours)	PETR	43.1%	1.320	54.2%	39.8%	189	13974	38463	49.4%	38.6%
TBQP-Baseline	PETRV2	44.2%	1.278	53.2%	41.7%	161	13328	38194	50.4%	41.0%
HSTrack (ours)	PETRV2	45.2%	1.274	56.6%	42.6%	192	13766	36290	51.1%	41.3%
PF-Track-F \dagger	PETR	45.0%	1.278	55.3%	42.5%	174	13116	35408	50.8%	41.8%
HSTrack (ours)	PETR	46.4%	1.262	56.9%	42.3%	204	12492	36417	51.0%	41.8%
CC-3DT (Fischer et al. 2022)	BEVFormer	41.0%	1.274	53.8%	35.7%	3334	-	-	-	-
DQTrack (Li et al. 2023c)	PETRV2	44.6%	1.251	-	-	1193	-	-	50.3%	41.0%
ADA-Track (Ding et al. 2024)	PETR	47.9%	1.246	60.2%	43.0%	767	15385	31402	-	-
PF-Track-F (Pang et al. 2023)	PETR	47.9%	1.227	59.0%	43.5%	181	16149	32778	51.4%	42.2%

Table 1: Comparison results on nuScenes val set. For a fair comparison, we divide the experiment into four groups based on the baseline settings. Our method is shown in light gray background. \dagger indicates we omit the Past reasoning module in PF-Track.

et al. 2020b), which consider multiple recall thresholds. nuScenes also uses secondary metrics from CLEAR MOT (Bernardin and Stiefelhagen 2008), including MOTA, MOTP, IDS (Identity Switches), FP (False Positive), and FN (False Negative), etc. We also report metrics of NDS (nuScenes detection score) and mAP (mean Average Precision) for detection to fully evaluate multi-task performance.

Baseline and implementation details

To assess the generalizability of our proposed hybrid supervision approach, we integrate HSTrack within several methods under the *track-by-query-propagation* paradigm, which extend different detectors to end-to-end trackers. Specifically, our experiments involve three query-based detectors: DETR3D (Wang et al. 2021), PETR (Liu et al. 2022), and PETRV2 (Liu et al. 2023). For DETR3D and PETR, we follow the experimental setups in ADA-Track (Ding et al. 2024) and PF-Track (Pang et al. 2023), respectively. Notably, PF-Track includes both a full resolution (1600×640 , indicated with "-F") and a small resolution (800×320 , indicated with "-S") setting. Due to GPU memory constraints, we reproduce PF-Track-F but omit the Past reasoning module. Regarding PETRV2, we establish the corresponding **TBQP-baseline** by substituting only the detector in the PF-Track-S framework. For the ablation studies, configurations of PF-Track-S are employed as the default. All models are initialized using pre-trained weights from single-frame detection training for 24 epochs and then we train our trackers on three-frame mini-samples. We adopt the AdamW (Loshchilov and Hutter 2019) optimizer with a weight decay of 1.0×10^{-2} . The learning rate is initially set to 2.0×10^{-4} and following a cosine annealing schedule.

Main results

We evaluate HSTrack on the nuScenes validation set. Tab. 1 presents the comparative results after integrating HSTrack into various trackers, with each baseline shown at the top

index	o2m	o2o	asso	AMOTA \uparrow	AMOTP \downarrow	Recall \uparrow
1				40.8%	1.343	50.7%
2	✓			41.8%	1.336	51.9%
3		✓		40.9%	1.339	52.0%
4	✓	✓		42.0%	1.337	52.0%
5	✓	✓	✓	43.1%	1.320	54.2%

Table 2: Ablation of hybrid supervision. "o2m", "o2o" and "asso" denote the one-to-many, one-to-one and associative supervision for track and object queries in U-decoder.

each of detector group. The experimental results based on the four baselines lead to four key observations: **1)** HSTrack can be adapted to various *tracking-by-query-propagation* paradigm methods, including MUTR3D and PF-Track. Specifically, HSTrack improves MUTR3D, PF-Track-S, PF-Track-F by +1.9%, +2.3%, and +1.4% AMOTA, respectively. **2)** HSTrack is compatible to various detectors, including PETR with regular attention, DETR3D with deformable attention and PETRV2 with temporal information. Building on our constructed TBQP-baseline, HSTrack achieves additional +1.0% and +0.7% boosts in AMOTP and NDS. This indicates that the issue of competition between track queries and object queries caused by self-attention is widespread in popular transformer-based decoders, and our hybrid supervision approach provides an effective solution. **3)** HSTrack enhances both detection and tracking performance, especially for models with lower resolution settings. For instance, HSTrack enables PF-Track-S to achieve a +1.7% NDS and +0.8% mAP improvement. **4)** HSTrack does not increase the number of false-positive predictions. On the contrary, it significantly reduces them. This is attributed to the one-to-many label assignment strategy for object queries in the parallel decoder without self-attention, facilitating the production of quality candidates by the tracker.

Query source	Matching Range	Strategy	Tracking				Detection		
			AMOTA↑	AMOTP↓	Recall↑	FP↓	FN↓	NDS↑	mAP↑
S-decoder	New-born ground-truth	one-to-many	39.0%	1.365	49.9%	12871	41667	46.8%	37.2%
U-decoder	All ground-truth	one-to-many	42.8%	1.316	53.2%	15044	37845	49.1%	38.6%
U-decoder	Consistent ground-truth	one-to-one	43.0%	1.317	53.9%	15605	37350	48.4%	38.7%
U-decoder	Consistent ground-truth	one-to-many	43.1%	1.320	54.2%	13974	38463	49.4%	38.6%

Table 3: Comparison results of different label assignment strategies for HSTrack.

Compared to the current state-of-the-art works, HSTrack with PETR at small resolution surpasses CC-3DT (Fischer et al. 2022) at full resolution using BEVFormer which has better detection performance by +2.0% AMOTA. Additionally, HSTrack outperforms DQTrack (Li et al. 2023c) following TBLA paradigm by +0.6% AMOTA and +0.8% NDS. The TBLA paradigm freezes the detector parameters, preventing simultaneous optimization for multi-task performance. By omitting the past reasoning module, HSTrack increases tracking speed and reduces false positives compared to ADA-Track. (Ding et al. 2024).

Ablation Studies

Efficacy of hybrid supervisions

In Tab. 2, we analyze the importance of each individual supervision in HSTrack for the model performance. Specifically, we decompose the hybrid supervision in the U-decoder into one-to-many supervision for object queries, one-to-one supervision for track queries and associative supervision. We observe that both one-to-many supervision (row 2) and one-to-one supervision (row 3) enhance overall tracking performance, with the former supervision providing greater benefits due to richer supervision signals, achieving 41.8% AMOTA. The latter supervision significantly improves the recall rate, which is beneficial for long-term modeling of track queries. The combination of these two supervision enables the model to achieve 42.0% AMOTA. Associative supervision (row 5) strengthens the connection and discrimination between object queries and track queries by encouraging the representations of matched positive query pairs to converge and negative query pairs to diverge, thereby further improving tracking performance by +1.1% in AMOTA. Together, these three types of supervision complement each other to effectively address the optimization challenges.

Label assignment strategies

In Tab. 3, we analyze the impact of different label assignment strategies for object queries on tracking and detection performance. We consider three different variants from the perspectives of query source, matching range, and matching strategy, compared to our baseline (highlighted in gray). First we explore whether the one-to-many matching strategy is applicable to standard decoders. Thus the first variant abandons the construction of the parallel U-decoder and directly migrates one-to-many supervision to object queries in S-decoder. It shows that directly increasing the number of supervision signals in the standard decoder instead de-

K	AMOTA↑	AMOTP↓	Recall↑	MOTA↑	IDS↓
2	41.6%	1.341	52.6%	38.9%	137
3	43.1%	1.320	54.2%	39.8%	189
4	42.3%	1.331	52.2%	39.4%	170

Table 4: Ablation of training sample lengths K .

grades tracking and detection performance, suggesting that the dispersing effect of self-attention tends to encourage object queries to match unique ground-truth targets. Duplicate matching relationships hinder model optimization. Second, we investigate whether object queries in the U-decoder can benefit from a broader matching range with ground-truth targets. The second variant extends the matching range from consistent ground-truth targets to all ground-truth targets. Compared to our baseline, it reduces the AMOTA and NDS by +0.3% and +0.3%, respectively. We infer that the cross-attention layers drive object queries to cluster towards track queries with feature priors, and thus the addition of new-born ground-truth targets is detrimental to the training of object queries in U-decoder. The third variant uses the Hungarian algorithm for one-to-one matching between object queries and consistent ground-truth targets. Although the tracking performance of this variant is comparable to our baseline, achieving 43.0% AMOTA, it reduces detection performance by +1% NDS and notably increases false-positive predictions. This suggests that one-to-one matching does not align well with the aggregation properties of cross-attention, leading to inaccurate predictions by object queries.

Frame Number for Training

In Tab. 4, we compare the tracking performance trained with different frame number K . We observe that when the frame number is increased from 2 to 3, HSTrack obtains a boost of +1.5% AMOTA. However, when $K > 3$, HSTrack cannot improve the model performance further. The reason is that more consecutive frames lead to more optimization objectives, making the training gradient increase and affecting the training stability. Considering the computational cost and performance, we use $K = 3$ as the default setting.

Conclusion

In this paper, we present HSTrack, an innovative approach to tackle the competitive optimization challenges between track and object queries in end-to-end camera-based 3D multi-object tracking. By leveraging auxiliary supervision

from a weight-sharing parallel decoder, HSTrack not only improves the quality of object query candidates and enhances the spatio-temporal modeling of track queries but also employs associative supervision, which fosters mutual learning between the queries, thereby optimizing both detection and tracking. Extensive experiments demonstrate the effectiveness of HSTrack, which can be seamlessly integrated into multiple trackers to improve multi-task performance.

References

- Bai, X.; Hu, Z.; Zhu, X.; Huang, Q.; Chen, Y.; Fu, H.; and Tai, C. 2022. TransFusion: Robust LiDAR-Camera Fusion for 3D Object Detection with Transformers. In *CVPR*, 1080–1089.
- Bernardin, K.; and Stiefelwagen, R. 2008. Evaluating Multiple Object Tracking Performance: The CLEAR MOT Metrics. *EURASIP J. Image Video Process.*
- Caesar, H.; Bankiti, V.; Lang, A. H.; Vora, S.; Liong, V. E.; Xu, Q.; Krishnan, A.; Pan, Y.; Baldan, G.; and Beijbom, O. 2020. nuScenes: A Multimodal Dataset for Autonomous Driving. In *CVPR*, 11618–11628.
- Carion, N.; Massa, F.; Synnaeve, G.; Usunier, N.; Kirillov, A.; and Zagoruyko, S. 2020. End-to-End Object Detection with Transformers. In *ECCV*, 213–229.
- Chen, Q.; Chen, X.; Wang, J.; Zhang, S.; Yao, K.; Feng, H.; Han, J.; Ding, E.; Zeng, G.; and Wang, J. 2023. Group DETR: Fast DETR Training with Group-Wise One-to-Many Assignment. In *ICCV*, 6610–6619.
- Dai, J.; He, K.; and Sun, J. 2016. Instance-Aware Semantic Segmentation via Multi-task Network Cascades. In *CVPR*, 3150–3158.
- Ding, S.; Rehder, E.; Schneider, L.; Cordts, M.; and Gall, J. 2023. 3DMOTFormer: Graph Transformer for Online 3D Multi-Object Tracking. In *ICCV*, 9750–9760.
- Ding, S.; Schneider, L.; Cordts, M.; and Gall, J. 2024. ADA-Track: End-to-End Multi-Camera 3D Multi-Object Tracking with Alternating Detection and Association. In *CVPR*.
- Doll, S.; Hanselmann, N.; Schneider, L.; Schulz, R.; Enzweiler, M.; and Lensch, H. P. A. 2024. S.T.A.R.-Track: Latent Motion Models for End-to-End 3D Object Tracking With Adaptive Spatio-Temporal Appearance Representations. *IEEE Robotics Autom. Lett.*, 1326–1333.
- Fischer, T.; Yang, Y.; Kumar, S.; Sun, M.; and Yu, F. 2022. CC-3DT: Panoramic 3D Object Tracking via Cross-Camera Fusion. In *CoRL*, 2294–2305.
- He, K.; Zhang, X.; Ren, S.; and Sun, J. 2016. Deep Residual Learning for Image Recognition. In *CVPR*, 770–778.
- Hu, H.; Yang, Y.; Fischer, T.; Darrell, T.; Yu, F.; and Sun, M. 2023a. Monocular Quasi-Dense 3D Object Tracking. *IEEE Trans. Pattern Anal. Mach. Intell.*, 1992–2008.
- Hu, Z.; Sun, Y.; Wang, J.; and Yang, Y. 2023b. DAC-DETR: Divide the Attention Layers and Conquer. In *NeurIPS*.
- Huang, J.; Huang, G.; Zhu, Z.; Ye, Y.; and Du, D. 2022. BEVDet: High-performance Multi-camera 3D Object Detection in Bird-Eye-View. *CoRR*, abs/2112.11790.
- Jia, D.; Yuan, Y.; He, H.; Wu, X.; Yu, H.; Lin, W.; Sun, L.; Zhang, C.; and Hu, H. 2023. DETRs with Hybrid Matching. In *CVPR*, 19702–19712.
- Jiang, B.; Luo, R.; Mao, J.; Xiao, T.; and Jiang, Y. 2018. Acquisition of Localization Confidence for Accurate Object Detection. In *ECCV*, 816–832.
- Kuhn, H. W. 2010. The Hungarian Method for the Assignment Problem. In *50 Years of Integer Programming*, 29–47. Springer.
- Lee, C.; Xie, S.; Gallagher, P. W.; Zhang, Z.; and Tu, Z. 2015. Deeply-Supervised Nets. In *AISTATS*.
- Lee, Y.; Hwang, J.; Lee, S.; Bae, Y.; and Park, J. 2019. An Energy and GPU-Computation Efficient Backbone Network for Real-Time Object Detection. In *CVPRW*, 752–760.
- Li, F.; Zhang, H.; Liu, S.; Guo, J.; Ni, L. M.; and Zhang, L. 2024. DN-DETR: Accelerate DETR Training by Introducing Query DeNoising. *IEEE Trans. Pattern Anal. Mach. Intell.*, 2239–2251.
- Li, Y.; Bao, H.; Ge, Z.; Yang, J.; Sun, J.; and Li, Z. 2023a. BEVStereo: Enhancing Depth Estimation in Multi-View 3D Object Detection with Temporal Stereo. In *Proceedings of the AAAI Conference on Artificial Intelligence*, 1486–1494.
- Li, Y.; Ge, Z.; Yu, G.; Yang, J.; Wang, Z.; Shi, Y.; Sun, J.; and Li, Z. 2023b. BEVDepth: Acquisition of Reliable Depth for Multi-View 3D Object Detection. In *Proceedings of the AAAI Conference on Artificial Intelligence*, 1477–1485.
- Li, Y.; Yu, Z.; Philion, J.; Anandkumar, A.; Fidler, S.; Jia, J.; and Alvarez, J. 2023c. End-to-end 3D Tracking with Decoupled Queries. In *ICCV*, 18256–18265.
- Li, Z.; Wang, W.; Li, H.; Xie, E.; Sima, C.; Lu, T.; Qiao, Y.; and Dai, J. 2022. BEVFormer: Learning Bird’s-Eye-View Representation from Multi-camera Images via Spatiotemporal Transformers. In *ECCV*, 1–18.
- Lin, T.; Goyal, P.; Girshick, R. B.; He, K.; and Dollár, P. 2020. Focal Loss for Dense Object Detection. *IEEE Trans. Pattern Anal. Mach. Intell.*, 318–327.
- Liu, Y.; Wang, T.; Zhang, X.; and Sun, J. 2022. PETR: Position Embedding Transformation for Multi-view 3D Object Detection. In *ECCV*, 531–548.
- Liu, Y.; Yan, J.; Jia, F.; Li, S.; Gao, A.; Wang, T.; and Zhang, X. 2023. PETRv2: A Unified Framework for 3D Perception from Multi-Camera Images. In *ICCV*, 3239–3249.
- Loshchilov, I.; and Hutter, F. 2019. Decoupled Weight Decay Regularization. In *ICLR*.
- Marinello, N.; Proesmans, M.; and Gool, L. V. 2022. Triplet-Track: 3D Object Tracking using Triplet Embeddings and LSTM. In *CVPRW*, 4499–4509.
- Pang, Z.; Li, J.; Tokmakov, P.; Chen, D.; Zagoruyko, S.; and Wang, Y. 2023. Standing Between Past and Future: Spatio-Temporal Modeling for Multi-Camera 3D Multi-Object Tracking. In *CVPR*, 17928–17938.
- Pang, Z.; Li, Z.; and Wang, N. 2022. SimpleTrack: Understanding and Rethinking 3D Multi-object Tracking. In *EC-CVW*, volume 13801, 680–696.
- Redmon, J.; and Farhadi, A. 2018. YOLOv3: An Incremental Improvement. *CoRR*, abs/1804.02767.

- Ren, S.; He, K.; Girshick, R. B.; and Sun, J. 2017. Faster R-CNN: Towards Real-Time Object Detection with Region Proposal Networks. *IEEE Trans. Pattern Anal. Mach. Intell.*, 1137–1149.
- Scheidegger, S.; Benjaminsson, J.; Rosenberg, E.; Krishnan, A.; and Granström, K. 2018. Mono-Camera 3D Multi-Object Tracking Using Deep Learning Detections and PMBM Filtering. In *IEEE Intelligent Vehicles Symposium*, 433–440.
- Sun, P.; Jiang, Y.; Zhang, R.; Xie, E.; Cao, J.; Hu, X.; Kong, T.; Yuan, Z.; Wang, C.; and Luo, P. 2020. TransTrack: Multiple-Object Tracking with Transformer. *CoRR*, abs/2012.15460.
- Wang, S.; Liu, Y.; Wang, T.; Li, Y.; and Zhang, X. 2023. Exploring Object-Centric Temporal Modeling for Efficient Multi-View 3D Object Detection. In *ICCV*, 3598–3608.
- Wang, Y.; Guizilini, V.; Zhang, T.; Wang, Y.; Zhao, H.; and Solomon, J. 2021. DETR3D: 3D Object Detection from Multi-view Images via 3D-to-2D Queries. In *Conference on Robot Learning*, 180–191. PMLR.
- Weng, X.; Wang, J.; Held, D.; and Kitani, K. 2020a. 3D Multi-Object Tracking: A Baseline and New Evaluation Metrics. In *IROS*, 10359–10366.
- Weng, X.; Wang, J.; Held, D.; and Kitani, K. 2020b. 3D Multi-Object Tracking: A Baseline and New Evaluation Metrics. In *IROS*, 10359–10366.
- Weng, X.; Wang, Y.; Man, Y.; and Kitani, K. M. 2020c. GNN3DMOT: Graph Neural Network for 3D Multi-Object Tracking With 2D-3D Multi-Feature Learning. In *CVPR*, 6498–6507.
- Weng, X.; Yuan, Y.; and Kitani, K. 2021. PTP: Parallelized Tracking and Prediction With Graph Neural Networks and Diversity Sampling. *IEEE Robotics Autom. Lett.*, 4640–4647.
- Wojke, N.; Bewley, A.; and Paulus, D. 2017. Simple online and realtime tracking with a deep association metric. In *ICIP*, 3645–3649.
- Yin, T.; Zhou, X.; and Krähenbühl, P. 2021. Center-Based 3D Object Detection and Tracking. In *CVPR*, 11784–11793.
- Zeng, F.; Dong, B.; Zhang, Y.; Wang, T.; Zhang, X.; and Wei, Y. 2022. MOTR: End-to-End Multiple-Object Tracking with Transformer. In *ECCV*, volume 13687, 659–675.
- Zeng, Y.; Ma, C.; Zhu, M.; Fan, Z.; and Yang, X. 2021. Cross-Modal 3D Object Detection and Tracking for Auto-Driving. In *IROS*, 3850–3857.
- Zhang, T.; Chen, X.; Wang, Y.; Wang, Y.; and Zhao, H. 2022a. MUTR3D: A Multi-camera Tracking Framework via 3D-to-2D Queries. In *CVPRW*, 4536–4545.
- Zhang, Y.; Sun, P.; Jiang, Y.; Yu, D.; Weng, F.; Yuan, Z.; Luo, P.; Liu, W.; and Wang, X. 2022b. ByteTrack: Multi-object Tracking by Associating Every Detection Box. In *ECCV*, 1–21.
- Zhang, Z.; Luo, P.; Loy, C. C.; and Tang, X. 2014. Facial Landmark Detection by Deep Multi-task Learning. In *ECCV*, 94–108.
- Zhou, X.; Wang, D.; and Krähenbühl, P. 2019. Objects as Points. *CoRR*, abs/1904.07850.
- Zhu, X.; Su, W.; Lu, L.; Li, B.; Wang, X.; and Dai, J. 2021. Deformable DETR: Deformable Transformers for End-to-End Object Detection. In *ICLR*.